

Incompressible Squeeze-Film Levitation

Mostafa A. Atalla,^{1,2,*} Ron A.J. van Ostayen,³ Aimée A. Sakes,¹ and Michaël Wiertlewski²

¹*BioMechanical Engineering Department, Delft University of Technology, The Netherlands*

²*Cognitive Robotics Department, Delft University of Technology, The Netherlands*

³*Precision and Microsystems Engineering Department, Delft University of Technology, The Netherlands*

(Dated: November 10, 2022)

Transverse vibrations can induce the non-linear compression of a thin film of air to levitate objects, via the squeeze film effect. This phenomenon is well captured by the Reynolds' lubrication theory, however, the same theory fails to describe this levitation when the fluid is incompressible. In this case, the computation predicts no steady-state levitation, contradicting the documented experimental evidence. In this letter, we uncover the main source of the time-averaged pressure asymmetry in the incompressible fluid thin film, leading the levitation phenomenon to exist. Furthermore, we reveal the physical law governing the steady-state levitation height, which we confirm experimentally.

When an object is placed in closed proximity to a surface vibrating at sufficiently high frequency, it levitates. Levitation has been exploited in a wide range of applications from squeeze-film bearings [1, 2], contactless manipulation and transportation of objects [3, 4] to friction-modulation in surface haptics touchscreens [5, 6].

In all those examples, levitation occurs when the surrounding fluid is air, which is compressible, via the so-called squeeze-film effect. Having the same ability to levitate objects in incompressible liquid environments could help bring non-contact manipulation and friction modulation to a range of applications, including the medical field where blood and liquids are omnipresent.

In-liquid levitation has been addressed by a limited number of studies. Hatanaka et al. [7] experimentally demonstrated that underwater near-field levitation is possible. Nomura et al. [8] realized a noncontact transportation underwater using ultrasonic traveling waves. However, neither of these studies provided an explanation of the physical underpinnings of this phenomenon, with the second speculating that it might be due to the non-linear viscosity of liquid. Tamura et al. [9] hypothesized that underwater levitation is due to formation of cavitation bubbles, which collapse at the surface of the levitated object. Although their experimental data matches well with their hypothesis, the relatively large experimental film thickness ($> 100 \mu\text{m}$) and high power ultrasonic transducer (350 W) limits the generality of their conclusion. This evidence indicates a gap in understanding the physical principles behind in-liquid levitation and thus, requires revisiting the existing theories.

The first leading theory that models squeeze film levitation is the Reynolds' lubrication theory [10]. This theory approaches the problem from the perspective of viscous fluids in a flow regime with negligible fluid inertia. Langlois [11] mathematically formalized the theory for the isothermal squeeze film case, which was later adopted and validated experimentally by Salbu [12] who showed that air squeeze films levitates mainly due to the non-linear compressibility of the viscous air film. Clearly, such an explanation is not applicable anymore once a liquid is used. As a consequence, employing the Reynolds equation to model the in-liquid levita-

tion phenomenon, fails and predicts no steady state levitation force. Based on this result, Stolarski et al. [13] believed that oil squeeze films have no load-carrying capacity. However, this theoretical result clearly contradicts the experimental evidence, which disqualifies the lubrication theory in its current form from modeling liquid squeeze film levitation.

The second leading theory in modeling squeeze film levitation is the acoustic radiation pressure theory. This theory takes the perspective of wave propagation in compressible inviscid fluids. The pioneering work of Chu and Apfel [14] shed the light on the radiation pressure of compression waves propagating through an elastic fluid medium in a confined space, acting on a perfectly reflecting surface. This fundamental work was adopted and simplified later by Hashimoto et al. [15] to model the special case of air thin films. Zhao et al. [16] showed experimentally, however, that this theory fails to capture the physics in air thin films of a typical thickness ($< 100 \mu\text{m}$), which was further confirmed by the experimental results of Li et al. [17]. This is mainly due to the fact that the viscous penetration depth (i.e. boundary layer thickness) is in the same order of magnitude of the film thickness, suggesting significant viscous effects which cannot be neglected [18]. The viscous effects of the boundary layer become even more significant in liquid whose viscosity is around two orders of magnitude higher than its air counterpart, which rules out the applicability of this theory to model the behaviour of liquid squeeze films.

A limited number of studies attempted to derive a unified viscoacoustic theory that works across the viscous and acoustic regimes. Melikhov et al. [19] developed a viscoacoustic model and identified the different operating regimes for air squeeze films as a function of the levitation height, confirming a purely viscous regime for typical squeeze film levitation systems. Ramanarayanan et al. [20] proposed another unified theory which described critical parametric conditions that causes levitation forces to switch to adhesion forces in air squeeze film systems. Remarkably, in the incompressible limit, their formulation predicted only weak adhesive squeeze film forces, adding even more uncertainty around the behaviour of incompressible squeeze films.

In other terms, the existing theories fail to capture the

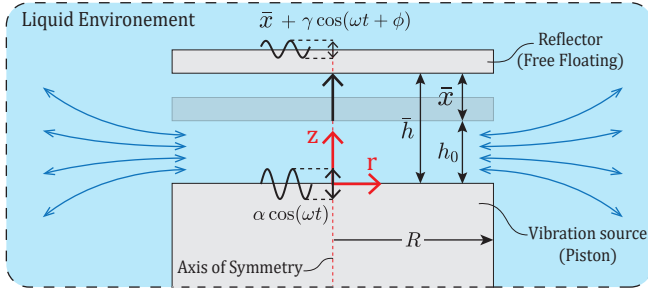


FIG. 1. In-liquid squeeze film levitation. Initially, a film thickness h_0 separates the vibrator and the free-floating reflector. This initial film thickness originates from various sources such as the roughness of the two surfaces or misalignment. Upon the start of the vibration $\alpha \cos(\omega t)$, a pressure builds up in the film layer, which pushes reflector away distance x until it reaches equilibrium at the time-averaged steady-state levitation distance \bar{x} . The reflector oscillates around its equilibrium position harmonically, denoted by $\gamma \cos(\omega t + \phi)$. The over-pressure in the liquid layer is linked to the steady state time-averaged levitation film height.

physics of liquid squeeze film levitation. We can also conclude that a viscous fluid approach (i.e. similar to the lubrication theory) is essential to tackle this problem given the comparable size of the film thickness and the boundary layer. However, relaxation of the assumptions of the lubrication theory is needed to uncover the underlying physics behind this phenomenon and find out its physical governing law.

In this letter, we show that a stable steady-state levitation of objects can be obtained in incompressible liquid environments at ultrasonic vibration frequencies. We uncover the fundamental pressure-inducing mechanisms in incompressible films. We reveal the physical law that governs the steady-state levitation height, which we validate experimentally. Finally, we compare the load-carrying capacity of liquid squeeze films with its air counterpart.

Consider an axisymmetric system of a sinusoidal vibration source, a free-floating reflector and a thin film of liquid in between as shown in Fig.1. We define the time-dependent film thickness $h(t)$ such that $h(0) = h_0$, where h_0 is an assumed initial film thickness between the source and reflector. The disc radius is R such that $R \gg h(t)$. The source oscillates with an angular frequency ω and an amplitude α such that $\alpha < h(t)$. We define the squeeze Reynolds number [21] to be $Re_s = \rho \omega \bar{h}^2 / \mu$ where \bar{h} is the steady-state time-averaged film thickness, ρ is the density of the liquid and μ is its viscosity. This number gives a measure of the relative significance of inertial and viscous effects.

One of the key assumptions of the lubrication theory is that fluid inertia is negligible and thus fluid behaviour is dominated by viscous effects. This proved to be true for gas squeeze films since the squeeze Reynolds number is typically less than unity (< 1) [22, 23]. However, in the case of a typical liquid, such as water, the order of magnitude of the physical parameters of the Reynolds number is as follows: $\rho \approx O(10^3)$, $\omega \approx O(10^4)$ and $\mu \approx O(10^{-3})$. Given the experimental data of Hatanaka

et al. [7], we can also expect the order of magnitude of (\bar{h}) to be $\bar{h} \approx O(10^{-5})$. This yields a Reynolds number of order $Re_s \approx O(10^1)$ suggesting the significance of the film inertia and thus, the lubrication theory's assumption becomes invalid. Therefore, we revisit the basic fluid governing equations, which take inertial effects into account.

Given the aforementioned axisymmetric system of a source and reflector and given that $R \gg h(t)$, we can safely assume that the pressure gradient across the film thickness is negligible compared to the radial pressure gradient ($\frac{\partial p}{\partial z} \ll \frac{\partial p}{\partial r}$) and therefore the pressure is only a function of the radial coordinate ($\frac{\partial p}{\partial z} = 0$). With this assumption, the conservation of momentum and mass equations for this system using cylindrical coordinates, are given by [24]:

$$\rho \left(\frac{\partial v_r}{\partial t} + v_r \frac{\partial v_r}{\partial r} + v_z \frac{\partial v_r}{\partial z} \right) = -\frac{\partial p}{\partial r} + \mu \frac{\partial^2 v_r}{\partial z^2} \quad (1)$$

$$\frac{1}{r} \frac{\partial}{\partial r} (r v_r) + \frac{\partial v_z}{\partial z} = 0 \quad (2)$$

where p is the liquid pressure, ρ is its density, μ is its viscosity, and v_r and v_z are the liquid velocity fields along r and z respectively. To solve for the pressure and velocity fields, the inertial forces (left hand side of Eq.1) can be approximated by employing the velocity profiles of the classical lubrication theory [25, 26], which are given by:

$$v_r = \frac{3r\dot{h}}{h^3} (z^2 - hz) \quad (3a)$$

$$v_z = -\frac{\dot{h}}{h^3} (2z^3 - 3hz^2) \quad (3b)$$

By integrating Eq.1 twice with respect to (z) and assuming static boundary conditions ($v_r(r, 0, t) = v_r(r, h, t) = 0$), we find the following expression for the radial velocity field (v_r):

$$v_r = \frac{1}{\mu} \frac{\partial p}{\partial r} \left(\frac{z^2}{2} - \frac{hz}{2} \right) + \frac{\rho}{\mu} \left[\frac{3r\ddot{h}}{h^3} \left(\frac{z^4}{12} - \frac{hz^3}{6} + \frac{h^3 z}{12} \right) + \frac{r\dot{h}^2}{h^6} \left(-\frac{z^6}{10} + \frac{3hz^5}{10} - \frac{3h^2 z^4}{4} + h^3 z^3 - \frac{9h^5 z}{20} \right) \right] \quad (4)$$

The conservation of mass principle requires that the inflow or outflow across the control volume of the film is equal to the volume change due to the source vibration and the reflector levitation. This condition can be expressed mathematically in integral form as follows:

$$\int_0^h v_r dz = -\frac{r\dot{h}}{2} \quad (5)$$

By substituting the velocity profile expression Eq.4 into the continuity equation Eq.5, we obtain the following expression for the pressure gradient along (r) :

$$\frac{\partial p}{\partial r} = \frac{6\mu r \dot{h}}{h^3} + \frac{3\rho r \ddot{h}}{5h} - \frac{15\rho r \dot{h}^2}{14h^2} \quad (6)$$

This expression of the pressure gradient has different coefficients of the second and third terms compared to the one presented by Li et al [27], because in that work the term $(v_z \frac{\partial v_r}{\partial z})$ was neglected. However, the magnitude of this term was previously shown to be comparable to $(v_r \frac{\partial v_r}{\partial r})$ [25]. By substituting Eq.6 back into Eq.4, we can obtain an improved expression for (v_r) which, in turn, can be substituted in Eq.2 to obtain a new expression for (v_z) . This iterative process can be repeated by substituting the new expressions of (v_r) and (v_z) into the left hand side of the momentum equation Eq.1 and then move through the same steps. However, Grimm et al. [28] previously concluded that this first order perturbation solution is stable and showed close agreement with the full numerical solution unlike the higher order perturbation solutions [29]. Thus, repeating the iterative scheme is of no benefit here. By integrating the pressure gradient expression with respect to (r) assuming the pressure boundary condition $(p(R,t) = p_a - \Delta p)$ where p_a is the ambient pressure and Δp is a pressure loss term due to the edge effect (to be discussed later), we obtain the following pressure field expression:

$$p - p_a = \frac{r^2 - R^2}{2} \left(\frac{6\mu\dot{h}}{h^3} + \frac{3\rho\ddot{h}}{5h} - \frac{15\rho\dot{h}^2}{14h^2} \right) - \Delta p \quad (7)$$

where $\Delta p = \begin{cases} \frac{C_e \rho R^2 h^2}{8h^2} & \text{if } \dot{h} > 0 \\ 0 & \text{otherwise} \end{cases}$

This pressure profile expression suggests three main pressure-inducing mechanisms for incompressible liquid films. The first one is associated with the viscosity of the liquid represented by the term $6\mu\dot{h}/h^3$. This term is symmetric and thus, has no contribution to the time-averaged pressure. The second and third mechanisms are associated with the temporal and convective accelerations of the liquid squeezing in and out of the thin film, represented by the asymmetric terms $3\rho\ddot{h}/5h$ and $15\rho\dot{h}^2/14h^2$ respectively. In addition, accounting for liquid inertia results in an inevitable pressure drop Δp at the edge of the squeeze film during negative squeeze motion ($\dot{h} > 0$), due to the sudden contraction of the liquid at the film entrance. Using Bernoulli's equation, we can find an expression for the pressure drop term [30, 31] equal to $C_e \rho R^2 \dot{h}^2 / 8h^2$ where C_e is a pressure loss coefficient that depends mainly on the geometry of the film entrance (i.e. sharp or round edge). This edge effect term along with the asymmetric temporal and convective acceleration terms contribute to a non-zero time-averaged pressure in the liquid film, thus clarifying that the in-liquid levitation phenomenon is driven by the inertial forces of the liquid (refer to the supplementary material [32] for more elaborate treatment of the pressure terms).

By looking closely at the pressure profile expression, we notice that the film pressure depends mainly on the time-varying film thickness $h(t)$ and its time derivatives \dot{h}, \ddot{h} . In a free-floating reflector context, the film thickness variables will depend on the relative motion between the source and reflector. Therefore, it is essential to couple the fluid dynamics with the dynamics of the levitated mass. The importance of

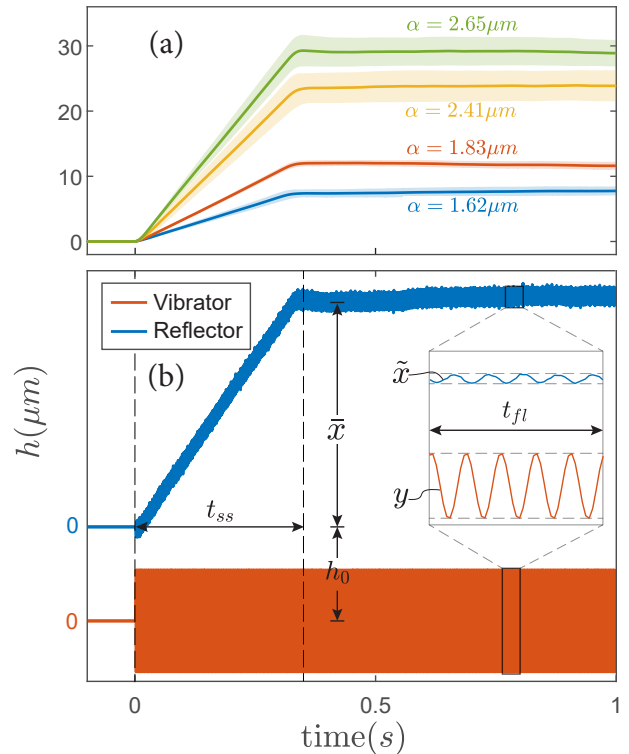


FIG. 2. (a) Demonstration of the stable steady-state levitation of a free floating reflector of mass 64g, that we can achieve under sinusoidal excitation of frequency 40kHz at different vibration amplitudes. For each vibration amplitude, five trials of measurements were collected and the results are plotted as the mean displacement (solid lines) and the standard deviation (shades). (b) A detailed view of one experimental trial corresponding to the input vibration amplitude $\alpha = 1.62\mu\text{m}$, with the vibrator's displacement being $y = \alpha \cos(\omega t)$. We observe that the floating mass levitates to a steady-state position \bar{x} and oscillates around the equilibrium position in response to the vibration input, where the oscillations are represented as \tilde{x} . We observe that the amplitude of the reflector oscillations is in the same order of magnitude as the input amplitude. The response also shows two characteristic time scales: (a) time corresponding to the mass reaching steady state levitation distance t_{ss} (b) time associated with the reflector oscillations around its equilibrium position t_{fl} .

dynamics coupling was also noted previously by Minikes et al. [33] who reported that the dynamics of the floating mass has significant influence on the behaviour of the fluid film. Incorporating the dynamics is also beneficial since for almost all applications (e.g. squeeze film bearings), the main interest is to levitate objects freely, not to fix their positions. Thus, predicting the levitation height directly is of paramount importance from an application perspective.

To incorporate the levitated object dynamics, we assume a single degree of freedom system where the reflector is a mass. The mass is connected to the vibrating surface through a liquid layer whose initial thickness is h_0 . We introduce two independent coordinates (x, y) where x is the displacement of the levitated object and y is the displacement of the vibrating sur-

face. The film height $h(t)$ is a function of x and y coordinates as follows:

$$h = h_o + x - y, \quad \dot{h} = \dot{x} - \dot{y}, \quad \ddot{h} = \ddot{x} - \ddot{y} \quad (8)$$

By analyzing the forces acting on the reflector, we can obtain its equation of motion and arrange the terms to get the following expression for its acceleration:

$$\ddot{x} = \left(\frac{10\dot{h}^2}{14h^2} - \frac{2\dot{y}}{5h} - \frac{4v\dot{h}}{h^3} - \frac{C_e\dot{h}^2}{4h^2} - Mg \right) / (M + \frac{2}{5h}) \quad (9)$$

$$\text{where } M = \frac{m}{\pi^2 R^4 \rho}, \quad v = \frac{\mu}{\rho}$$

where the mass ratio (M) is the ratio of the mass per unit area of the levitated object, to the mass per unit height of the liquid film. It is a measure of the relative significance of the inertial effects of the free floating object and the liquid film. The kinematic viscosity (v), on the other hand, is a measure of the fluid resistance to flow under inertial forces.

To understand the nature of this dynamical system, we conducted initial experiments in which we measured the levitation displacement of a free floating mass placed on top of a vibrating surface in a liquid container, in a fashion similar to other experiments from literature [33–35]. To find the actual capacity of liquid squeeze films to levitate objects stably, we tested the system under ultrasonic sinusoidal excitation of frequency 40 kHz at different vibration amplitudes. As demonstrated in Fig.2(a) for a mass of (64 g), experiments confirmed the existence of stable squeeze-film levitation in liquid. To further investigate whether cavitation bubbles play a role in this phenomenon in light of the hypothesis of Tamura et al. [9], we visualized the surface area of the liquid film subjected to the sinusoidal excitation and we found no trace of bubbles in our experiments using a purified liquid (refer to the supplementary material [32] for details about the experimental setup).

By looking closely at the response shown in Fig.2(b), we observe the following: the reflector reaches an equilibrium levitation position while oscillating in response to the input excitation. We notice that the amplitude of the reflector oscillations is considerably smaller than the input amplitude ($\approx 15\%$), indicating that the reflector oscillations has a minor influence on the squeeze film pressure compared to the input vibration. In addition, we also find the phase shift between the reflector oscillations and input vibrations to be around ($\frac{\pi}{2}$), consistent across experiments. Finally, the dynamic response of the system has two characteristic time scales: (a) a time corresponding to the mass reaching a steady-state levitation position t_{ss} (b) a time associated with the reflector oscillations around its equilibrium position t_{fl} , such that ($t_{ss} \gg t_{fl}$). Since, we are mainly interested in the steady-state time-averaged levitation, we can exploit this observation to decompose the response into two components; namely, a time-averaged and an oscillating components as follows:

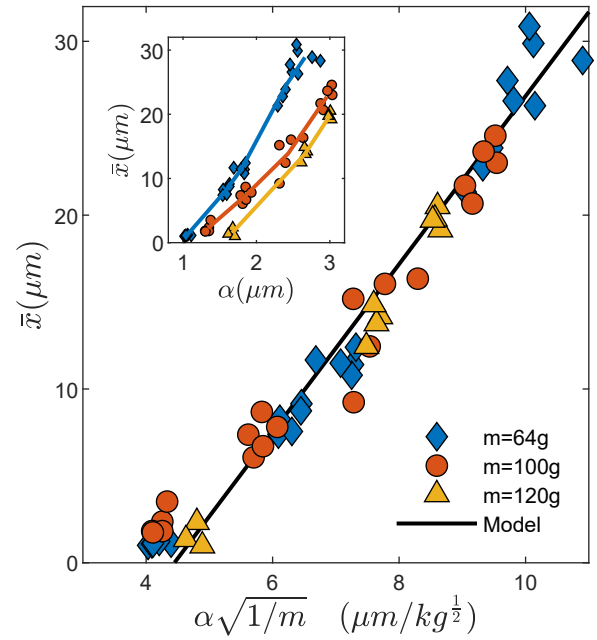


FIG. 3. Validation of the model demonstrated by the steady-state time-averaged levitation height \bar{h} as a function of the vibration amplitude and mass of the reflector expressed as $\alpha\sqrt{1/m}$. The experimental data were collected using three different masses: 64 g (blue parallelograms), 101 g (orange circles) and 122 g (yellow triangles) at vibration amplitudes up to $3\mu\text{m}$. The model (black solid line) shows close agreement with the experimental data (individual plotted points) at different combinations of vibration amplitudes and masses. We identified the initial film thickness h_0 to be $\approx 22\mu\text{m}$ and the pressure loss coefficient C_e to be ≈ 9 . The inset shows the decomposed experimental data; the steady-state time-averaged levitation height \bar{h} as a function of the vibration amplitude α for each mass individually.

$$x = \bar{x} + \tilde{x} = \bar{x} + \gamma \cos(\omega t + \phi) \quad (10)$$

where \bar{x} is the time-averaged steady-state levitation distance and \tilde{x} is the oscillation component such that $\tilde{x} = \gamma \cos(\omega t + \phi)$. A similar decomposition was previously proposed by Wang et al.[35]. However, in that work, the decomposed parameter was the squeeze film force, not the levitation displacement. By substituting Eq.10 into Eq.8, we can find new expressions for the film thickness $h(t)$ incorporating the decomposition components. Since we are mainly interested in the time-averaged levitation component (\bar{x}), we can impose a time average operator $\langle \cdot \rangle$ on the dynamic equation Eq.9 to find the steady-state time-averaged components. This time average operator is given by $\langle \cdot \rangle = \frac{1}{T} \int_0^T \cdot dt$, where T is the period of the oscillation. To be able to compute the analytical time average of the components of Eq.9, it is essential that the integral of these components using the time average operator to exist. This turns out to be true in the special case when the mass ratio M is negligible compared to the $\frac{2}{5h}$ term in the denominator of the right hand side of Eq.9. To find the range of values

where the assumption of a negligible mass ratio is valid, we carry out an order of magnitude study: for masses of few hundred grams $O(10^{-1})$, radii of tenth of millimeters $O(10^{-2})$ and for a typical liquid density of order $O(10^3)$, we find the order of magnitude of the mass ratio to be $O(10^3)$ compared to an $O(10^5)$ for the $\frac{2}{5h}$ term. Therefore, we can safely conclude that the assumption we made priori (i.e. $M \ll \frac{2}{5h}$) is valid for the aforementioned ranges of values of mass, radii and density. By imposing this assumption on Eq.9, we obtain the following expression:

$$\ddot{x} = \frac{25\dot{h}^2}{14h} - \ddot{y} - \frac{10v\dot{h}}{h^2} - \frac{5C_e\dot{h}^2}{8h} - \frac{5hMg}{2} \quad (11)$$

A remarkable consequence of the $M \ll \frac{2}{5h}$ assumption is that all of the terms of Eq.9 become symmetric in Eq.11 except for the convection terms $\frac{25\dot{h}^2}{14h}$ and $\frac{5C_e\dot{h}^2}{8h}$. It means that within the range of values in which the assumption is valid, the convection effects prevail and becomes the sole source of the steady-state time-averaged levitation. By imposing the time average operator, the symmetric terms \ddot{x} , \ddot{y} and $\frac{10v\dot{h}}{h^2}$ of Eq.11, by definition, converge to zero which yields the following:

$$\langle \dot{h}^2 \rangle = \frac{(20 - 2.2C_e)}{28Mg} \langle \dot{h}^2 \rangle \quad (12)$$

The time average of the film height yields the steady-state component \bar{h} which is the main variable that we are trying to find here. On the other side of the equation, we can find the time average of the \dot{h}^2 by substituting the derivative of Eq.10 into the \dot{h} expression of Eq.8 and find the time average integral, to be:

$$\langle \dot{h}^2 \rangle = \frac{\alpha^2 \omega^2}{2} + \frac{\gamma^2 \omega^2}{2} - \alpha \gamma \omega^2 \cos(\phi) \quad (13)$$

Given our earlier experimental findings that the amplitude of the reflector oscillations is typically ($\gamma \leq \frac{\alpha}{6}$) and that the phase shift is consistently ($\phi \approx \frac{\pi}{2}$), we can conclude that the reflector dynamics terms $\gamma^2 \omega^2/2$ and $\alpha \gamma \omega^2 \cos(\phi)$ are negligible compared to the vibration input term $\alpha^2 \omega^2/2$. By omitting the negligible terms from Eq.13, substituting it back in Eq.12 and expanding the mass ratio M , we find the following expression for the time-averaged steady-state film height \bar{h} :

$$\bar{h} = \pi R^2 \alpha \omega \Phi \sqrt{\frac{\rho}{mg}} \quad (14)$$

where $\Phi(C_e)$ is a correction factor that encapsulates the energy dissipation due to the edge effect, such that $\Phi = \sqrt{(20 - 2.2C_e)/56}$. The derived physical law reveals the fundamental relationship between the steady-state time-averaged levitation height and the system parameters in the case of prevailing convection effects. In comparison to the derived formula by Wang et al.[35] for in-air levitation, we see that \bar{h}

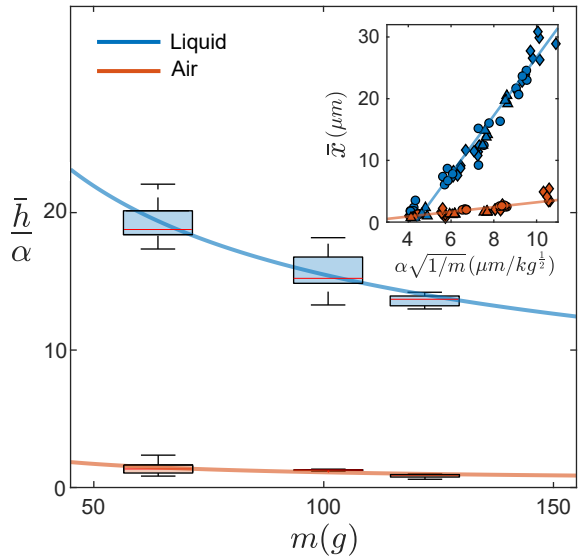


FIG. 4. A comparison of the load-carrying capacity between the in-liquid and in-air levitation, demonstrated by the box-plot of the amplification factor $\frac{\bar{h}}{\alpha}$ as a function of the mass of the floating reflector where the solid lines are power law regression. The comparison shows that at the same mass, the in-liquid system achieves a significantly greater amplification than the levitation in air. The inset shows the steady state levitation distances \bar{x} of the in-liquid and in-air levitation at different combinations of vibration amplitudes and masses, indicating that both incompressible liquids and air follow a linear relationship with $\alpha \sqrt{1/m}$, but with different slopes, as expected from our model for the liquid case and the literature for the air case.

scales linearly in both cases with the vibration amplitude α and with the inverse of the square root of the mass $\sqrt{1/m}$. By contrast, in the liquid case, \bar{h} is proportional to the surface area πR^2 , the angular frequency ω and the square root of the liquid density $\sqrt{\rho}$ while in the air case, \bar{h} is proportional to the square root of the surface area $\sqrt{\pi R^2}$ and has no direct relation with the angular frequency nor with the density. These differences are well justified by the fundamental difference between the working mechanism of in-air (compressibility) and that of in-liquid systems (inertial).

To validate the theory, we conducted experiments using different combinations of masses (64, 101 and 122 g) with a disk of radius (10 mm) and ultrasonic (40 kHz) vibration amplitudes (1-3 μm), in a purified liquid of density (1030 kg/m^3). Given the relative scaling between the surface area πR^2 and the input vibration angular frequency ω in Eq.14, we notice that for our disk size $O(10^{-2})$, it was necessary to have an ultrasonic excitation of angular frequency $\omega O(10^5)$ to obtain a measurable levitation height.

Using the collected experimental data, we identified the empirical parameters (h_0, C_e) to be $h_0 \approx 22\mu\text{m}$ and $C_e \approx 9$. As demonstrated in Fig.3, the model shows close agreement with the experimental data. We also observe that the correction factor Φ is not influenced by the vibration amplitude nor the mass, as expected, since the loss coefficient, by definition, de-

pends only on the geometry of the film entrance. In addition, it is interesting to see that levitation starts to occur at certain amplitude threshold which mainly stems from the initial gap thickness h_0 , as expected from our model. The observation was also noted for air squeeze films [35]. This effect is mainly because for thicker squeeze films, higher amplitude is required to induce sufficient pressure in the film to outweigh the mass of the reflector and vice versa.

Since air squeeze levitation systems is the de facto standard in the literature, we conducted the same set of experiments in air. As demonstrated in Fig. 4, we see that the amplification factor $\frac{\bar{h}}{\alpha}$, which is the ratio of the steady-state levitation height to the amplitude of the input vibration, is significantly higher in liquid compared to air across different masses, reaching levitation amplification ten times larger in the liquid case. We also observe that while both liquid and air scales linearly with $\alpha\sqrt{1/m}$, the slope in both cases is different. The slope in the liquid case is around ten times greater than the air case. The difference in slope demonstrates the significantly greater load-carrying capacity of liquid squeeze films compared to air, based solely on the squeeze film effect.

In summary, we showed for the first time that the liquid inertia, manifested as the temporal and convective acceleration of the liquid film, is the source of pressure asymmetry that causes the levitation phenomenon to exist. We demonstrated that in the special case of a negligible mass ratio (M) compared to a film thickness parameter ($\frac{2}{5}h$), the fluid convective inertial effects prevail and become the sole source of the levitation phenomenon. In such a case, we simplified the dynamics equation and we derived a closed form compact formula that predicts the steady-state time-averaged levitation height as a function of the vibration input parameters (α, ω), liquid density (ρ) and mass (m) of the levitated object. In addition, we demonstrated the true capacity of liquid squeeze films to carry loads stably under periodic input excitation, confirming earlier published results. Lastly, we conducted a comparative experiment of load carrying capacity of liquid and air squeeze film levitation systems, demonstrating a significantly greater load-carrying capacity for in-liquid systems. The findings of this letter could potentially lead to novel physics-informed designs of in-liquid levitation systems for non-contact manipulation, transportation and friction modulation applications.

- [4] R. Gabai, R. Shaham, S. Davis, N. Cohen, and I. Bucher, A Contactless Stage Based on Near-Field Acoustic Levitation for Object Handling and Positioning-Concept, Design, Modeling, and Experiments, *IEEE/ASME Transactions on Mechatronics* **24**, 1954 (2019).
- [5] L. Winfield, J. Glassmire, J. E. Colgate, and M. Peshkin, T-PaD: Tactile pattern display through variable friction reduction, *Proceedings, IEEE World Haptics 2007*, 421 (2007).
- [6] M. Wiertlewski, R. F. Friesen, and J. E. Colgate, Partial squeeze film levitation modulates fingertip friction, *Proceedings of the National Academy of Sciences of the United States of America* **113**, 9210 (2016).
- [7] T. Hatanaka, Y. Koike, K. Nakamura, S. Ueha, and Y. Hashimoto, Characteristics of underwater near-field acoustic radiation force acting on a planar object, *Japanese Journal of Applied Physics, Part 2: Letters* **38**, 6 (1999).
- [8] S. Nomura, T. J. Matula, J. Satonobu, and L. A. Crum, Non-contact transportation in water using ultrasonic traveling waves, *The Journal of the Acoustical Society of America* **121**, 1332 (2007).
- [9] S. Tamura, Y. Tsunekawa, and M. Okumiya, Effect of ultrasonic cavitation on force acting on solid object in water, *Japanese Journal of Applied Physics, Part 1: Regular Papers and Short Notes and Review Papers* **45**, 2842 (2006).
- [10] O. Reynolds, On the Theory of Lubrication and Its Application to Mr. Beauchamp Tower's Experiments, *Philosophical Transactions of the Royal Society of London* **177**, 157 (1886).
- [11] W. E. Langlois, Isothermal Squeeze Films, *Quarterly of Applied Mathematics*, **53**, 1689 (1962).
- [12] E. O. J. Salbu, Compressible Squeeze Films and Squeeze Bearings, *Journal of Basic Engineering* **86**, 355 (1964).
- [13] T. A. Stolarski and W. Chai, Load-carrying capacity generation in squeeze film action, *International Journal of Mechanical Sciences* **48**, 736 (2006).
- [14] B. T. Chu and R. E. Apfel, Acoustic radiation pressure produced by a beam of sound, *Journal of the Acoustical Society of America* **72**, 1673 (1982).
- [15] Y. Hashimoto, Y. Koike, and S. Ueha, Near-field acoustic levitation of planar specimens using flexural vibration, *The Journal of the Acoustical Society of America* **100**, 2057 (1996).
- [16] S. Zhao, S. Mojrzisch, and J. Wallaschek, An ultrasonic levitation journal bearing able to control spindle center position, *Mechanical Systems and Signal Processing* **36**, 168 (2013).
- [17] R. Li, Y. Li, H. Sang, Y. Liu, S. Chen, and S. Zhao, Study on near-field acoustic levitation characteristics in a pressurized environment, *Applied Physics Letters* **120**, 10.1063/5.0075193 (2022).
- [18] M. A. Andrade, T. S. Ramos, J. C. Adamowski, and A. Marzo, Contactless pick-and-place of millimetric objects using inverted near-field acoustic levitation, *Applied Physics Letters* **116**, 10.1063/1.5138598 (2020).
- [19] I. Melikhov, S. Chivilikhin, A. Amosov, and R. Jeanson, Viscoacoustic model for near-field ultrasonic levitation, *Physical Review E* **94**, 1 (2016).
- [20] S. Ramanarayanan, W. Coenen, and A. Sánchez, Viscoacoustic squeeze-film force on a rigid disk undergoing small axial oscillations, *Journal of Fluid Mechanics* **933**, A15 (2022).
- [21] N. Brunetière and M. Wodtke, Considerations about the applicability of the Reynolds equation for analyzing high-speed near field levitation phenomena, *Journal of Sound and Vibration* **483**, 1 (2020).
- [22] A. Minikes, I. Bucher, and S. Haber, Levitation force induced by pressure radiation in gas squeeze films, *The Journal of the Acoustical Society of America* **116**, 217 (2004).

* Corresponding author.
m.a.a.atalla@tudelft.nl

- [1] M. Wiesendanger, Squeeze film air bearings using piezoelectric bending elements (2001).
- [2] T. Ide, J. R. Friend, K. Nakamura, and S. Ueha, A Low-Profile Design for the Noncontact Ultrasonically Levitated Stage, *Japanese Journal of Applied Physics* **44**, 4662 (2005).
- [3] S. Ueha, Y. Hashimoto, and Y. Koike, Non-contact transportation using near-field acoustic levitation, *Ultrasonics* **38**, 26 (2000).

- [23] T. A. Stolarski and W. Chai, Inertia effect in squeeze film air contact, *Tribology International* **41**, 716 (2008).
- [24] B. J. Hamrock and S. R. Schmid, *Fundamentals of Fluid Film Lubrication Second Edition* (CRC Press, 2004) pp. 1–693.
- [25] D. C. Kuzma, Fluid inertia effects in squeeze films, *Appl. Sci. Res.* **18**, 15 (1967).
- [26] J. D. Jackson, A Study of Squeezing Flow, *Appl. Sci. Res.* **11**, 148 (1963).
- [27] J. Li, W. Cao, P. Liu, and H. Ding, Influence of gas inertia and edge effect on squeeze film in near field acoustic levitation, *Applied Physics Letters* **96**, 1 (2010).
- [28] R. J. Grimm, Squeezing flows of Newtonian liquid films an analysis including fluid inertia, *Applied Scientific Research* **32**, 149 (1976).
- [29] J.A. Tichy and W.O. Winer, Inertial Considerations in Parallel Circular Squeeze Film Bearings, *ASME Pap* , 588 (1970).
- [30] H. Hashimoto, Squeeze Film Characteristics Between Parallel Circular Plates Containing a Single Central Air Bubble in the Inertial Flow Regime, *Journal of Tribology* **117**, 513 (1995).
- [31] Squeeze film, in *Hydrodynamic Lubrication* (Springer Tokyo, Tokyo, 2006) pp. 137–160.
- [32] See supplemental material at [url will be inserted by publisher] for more details about the experimental setup, analysis and fem simulation.
- [33] A. Minikes and I. Bucher, Coupled dynamics of a squeeze-film levitated mass and a vibrating piezoelectric disc: Numerical analysis and experimental study, *Journal of Sound and Vibration* **263**, 241 (2003).
- [34] P. Liu, J. Li, H. Ding, and W. Cao, Modeling and experimental study on near-field acoustic levitation by flexural mode, *IEEE Transactions on Ultrasonics, Ferroelectrics, and Frequency Control* **56**, 2679 (2009).
- [35] Y. Wang and P. Guo, Stiffness modeling for near field acoustic levitation bearings, *Applied Physics Letters* **118**, 10.1063/5.0051372 (2021).